Wood Science and Technology
https://doi.org/10.1007/s00226-024-01596-5

ORIGINAL

Mechanistic insight into hydroxy-methylation of hardwood Kraft lignin

Micaela B. Peralta[1,2] · Nicolò Pajer[3,4] · Claudia Crestini[3,4] · Verónica V. Nicolau[1,2]

Received: 21 May 2024 / Accepted: 22 August 2024

Abstract

In view of developing upcycling strategies for hardwood Kraft lignin, hydroxy-methylation of Eucalyptus Kraft lignin under alkaline conditions (pH 9 and 11) at different temperatures (50 °C and 70 °C) was studied in the present effort with the double objective of optimizing the reaction conditions and understanding the functionalization mechanism of C_5 in either terminal or internal guaiacyl units during hydroxy-methylation. Formaldehyde consumption was estimated via titration of the oximated free formaldehyde; the hydroxy-methylation degree under the reaction was estimated by calculating the ratio in Condensed hydroxyl/Guaiacyl (Condensed OH/G-OH) via a new difference UV-spectroscopy. The reliability of the difference UV-method results for the analyses of the hydroxy-methylated lignins was statistically analysed and compared with that of vacuum-dried and sonicated samples. Hydroxy-methylated samples were then fully characterised by NMR (^{31}P and HSQC) and GPC. The reaction temperature of 50 °C, pH 11, and period time of one hour resulted as the optimal conditions for the hydroxy-methylation, preventing the side-reactions leading to the formation of dimethylene-glycol addition products. The ^{31}P and ^{1}H–^{13}C HSQC NMR revealed the absence of undesirable formaldehyde *Cannizzaro* by-products and the lack of hydroxymethyl groups in the aliphatic side chain under the studied conditions. GPC analyses, comparing two methodologies, revealed increases in molar mass of the hydroxy-methylated samples upon the formaldehyde addition. The selective hydroxy-methylation at the C5 guaiacyl site demonstrates that Eucalyptus Kraft lignin is as a promising candidate for resol production.

Introduction

Despite its heterogeneity, low solubility, and low reactivity, the interest of both industry and academia in valorising Kraft lignin (KL), an underutilized resource, has increased in recent years (Argyropoulos et al. 2023). As of now, pulping industry relies on either softwood or hardwood feedstock; in particular, the pulping of

Extended author information available on the last page of the article

Published online: 24 September 2024

Eucalyptus spp. species plays a vital role as the primary fibre source for the pulp and paper industry in South America (Vallejos et al. 2017). Softwood and hardwood KL differ in their chemical structure; while softwood KL consists almost exclusively of guaiacyl units, hardwood KL contains both guaiacyl and syringyl units. Of the two, softwood is the one which best fits for the preparation of phenolic resins, polyurethanes, and epoxy resins due to its higher reactivity (Kun & Pukánszky 2017). The presence of syringyl units in hardwood KL reduces its reactivity due to the reduced content in C5-position suitable for nucleophilic attack generating KL-derivatives.

Hydroxy-methylation, also known as methylolation, represents the most frequently employed strategy for activating lignin; in fact, by treating lignin with formaldehyde (F, CH_2O) under heat and alkaline conditions it is possible to introduce hydroxymethyl groups ($–CH_2OH$) that can participate in future condensation reactions suitable to produce adhesives, polyurethanes and resins (Chen et al. 2020; El Mansouri et al. 2018).

The hydroxy-methylation of lignins has been studied on many occasions at temperatures between 40 °C (Olivares et al. 1988) and 150 °C (Paananen & Pakkanen 2020) under alkaline conditions, with 50 °C (Peng et al. 1993; Zhao et al. 1994; Vázquez et al. 1997; Vázquez et al. 1999; Alonso et al. 2001; Malutan et al. 2008; El Mansouri et al. 2011, 2018; Taverna et al. 2015; Taverna et al. 2017) and 70 °C (Muller & Glasser 1984; Dilling, 1987; Kuo et al. 1991; Taverna et al. 2019) being the most studied conditions. Under alkaline conditions, F predominantly attacks the C_5 position of the lignin aromatic ring via the *Lederer – Manasse* reaction, and to a lesser extent, the propanoic side chain, typically adjacent to a carbonyl group in C_β or at the beta carbon of an $C_\alpha C_\beta$ double bond. Harsh reaction conditions, as a strong alkalinity ($pH > 10$) or high temperature, lead to the undesirable *Cannizzaro* side reaction, where F undergoes deprotonation with generation of methanol and formic acid, resulting in the consumption of the reagent (Campbell & Walsh 1985; Malutan et al. 2008; Taverna et al. 2019).

In order to produce resols, pivotal in adhesives or composites production, the introduction of $-CH_2OH$ in the aromatic ring is the only desirable reaction. However, for the synthesis of polyols suitable to produce polyurethane, the addition of $-CH_2OH$ onto either aliphatic or aromatic domains is desirable.

Another reaction that can easily occur during lignin hydroxy-methylation involves the formation of methylene groups binding aromatic rings; in particular, by increasing the temperature, $-CH_2OH$ groups on an aromatic ring can react with other free vicinal C_5 in guaiacyl units, generating the methylene bonds which result in a reduction of the hydroxy-methylated content, an increase in the condensation degree of KL, and an increase in the overall molecular weights (Aini et al. 2019; Malutan et al. 2008).The application of hydroxy-methylation on softwood KL to produce resols in wood binders and resins has been widely investigated, especially at strong alkalinity (Kuo et al. 1991; Zhao et al. 1994). It was demonstrated that the synthesis of resols for wood applications is efficiently performed at pH 12 to ensure the water solubility of the resulting resol as well as a high condensation degree. Differently, for impregnation applications such as the production of high-pressure laminates, resol synthesis is commonly performed under mildly alkaline conditions ($pH = 9$) until oligomers become immiscible

in water; then, water is removed under vacuum and alcohol is used as a diluent (Nicolau et al. 2013).

In view of that, the identification of the optimal hydroxy-methylation conditions is crucial for developing tailor-made formulations based on hardwood KL, a still underexploited resource, to conveniently choose between one- or two-stage processes. In a one stage process, lignin, phenol, and F are mixed from the beginning of the reaction, while in a two-stage process lignin is pre-hydroxy-methylated and then phenol is added in a second stage (El Mansouri et al. 2018; Taverna et al. 2019).

The structural features of hydroxy-methylated lignins and their derivates can be conveniently investigated via ^{13}C and ^{31}P nuclear magnetic resonance (NMR) techniques, which provide reliable results in an academic perspective; moreover, these approaches imply the utilization of expensive equipment, especially while monitoring reactions in the industry (Paananen et al. 2021). The fast and simple difference UV-spectroscopic method, based on the change in absorbance when phenolic hydroxyl groups (*ph*–OH) are ionized in an alkaline condition (Gärtner et al. 1999; Ruwoldt et al. 2022) is a much more convenient strategy for the *on-line* monitoring of a reaction mixture. The major drawback of the UV-method relies on the need of soluble lignin preparations at either pH = 6 or pH = 12–13 (Ruwoldt et al. 2022). However, as the incorporation of $-CH_2OH$ groups in lignin enhances its solubility in a wide range of pH, this limitation is easily overcome for hydroxy-methylated samples.

In the present paper, the identification of the optimal conditions for promoting hardwood KL hydroxy-methylation is reported. Additionally, the reliability of the aqueous difference UV-spectroscopic method for following the progress of the Condensed OH/G-OH ratio along the hydroxy-methylation, as well as for characterising the resulting hydroxy-methylated KL has been investigated. Furthermore, the typical gel permeation chromatography (GPC) analyses in dimethyl-sulfoxide (DMSO) used for the characterization of lignins was compared to the typical GPC in dimethylformamide (DMF) widely employed in the separation and characterization of polar F resins and polyurethanes with varying degrees of branching, crosslinking, or functional groups. By using more than one method, results can be cross-verified, enhancing the accuracy and reliability of molecular weight determination.

The kinetic of hardwood KL hydroxy-methylation at different pH (9 and 11) and temperatures (50 °C and 70 °C) was monitored using a volumetric technique capable of estimating the F consumption, while the F up-take was estimated via difference UV-spectroscopy. The reliability of the difference UV-method was statistically analysed by comparing vacuum-drying, sonicated and untreated liquefied hydroxy-methylated samples. The resulting hydroxy-methylated samples were fully characterised via NMR and GPC methods.

Materials and methods

Lignin characterisation and hydroxy-methylation reactions

Eucalyptus KL was supplied by Suzano S.A. (Brazil) with 3.58% humidity and 2.37% ash content.

Hydroxy-methylation experiments were performed at 50 °C and 70 °C at pH 9 and 11 at constant weight ratio F/KL = 1. Reaction conditions are summarised in Table 1. Reactions were performed in triplicate, in a 500 mL three-neck round-bottom flask equipped with mechanical stirring.

The flask was loaded with 37 wt. % F aqueous solution and the pH was adjusted by addition of 34 wt. % NaOH aqueous solution. Then, pulverized KL was added under vigorous stirring; the pH was re-adjusted. The temperature was gradually raised at 1.6 °C min^{-1} to the desired value (zero time), then the mixture was kept under heating and stirring for 4 h. To estimate the F consumption deriving from the *Cannizzaro* reaction or potential losses deriving from the lack of tightness of the equipment, all experiments were replicated in triplicate without the addition of KL (control reactions). During the hydroxy-methylation reaction and control tests the total free F was measured by the volumetric oximation method based on the reaction of F with hydroxylamine hydrochloride. Additionally, a difference UV-absorption spectroscopic method was fine-tuned for measuring the Condensed OH/G-OH ratio during hydroxy-methylation experiments. The KL and final hydroxy-methylated KL were dried under vacuum at 40 °C, and analysed via GPC, ^{31}P NMR and HSQC. Two different GPC methodologies were compared.

Measurements

Oximation method (ISO 11402:2004)

For the estimation of free F about 1.5 g of the sample were dissolved in 50 mL of water and the pH was adjusted to 4 using 0.1 M and 1 M HCl. Then, 15 mL of 10 wt. % hydroxylamine hydrochloride aqueous solution were added under mild stirring for 10 min. The resulting solution was then titrated with 1 M NaOH solution up to pH 4.

Table 1 Hydroxy-methylation: Recipes and reaction conditions. F/KL = 1

	Exp. 1	Exp. 2	Exp. 3	Exp. 4
Reaction conditions:				
	50 °C	70 °C	50 °C	70 °C
	pH 9 ± 0.5	pH 9 ± 0.5	pH 11 ± 0.5	pH 11 ± 0.5
Hydroxy-methylation initial concentrations:				
[F]°, mol L^{-1}	9.43 ± 0.00	9.39 ± 0.01	9.06 ± 0.02	9.04 ± 0.02
KL°, g L^{-1}	283 ± 0.01	283 ± 0.01	273 ± 0.01	271 ± 0.01
[NaOH]°, mol L^{-1}	0.29 ± 0.00	0.33 ± 0.02	0.64 ± 0.03	0.67 ± 0.03
[H_2O]°, mol L^{-1}	28.02 ± 0.01	28.05 ± 0.05	28.49 ± 0.07	28.52 ± 0.04

Difference UV

Total *ph*-OH was determined via Ultraviolet Ionization Difference Spectrophotometry (Δε-method) using a double beam UV–Vis Perkin Elmer Spectrophotometer Model Lambda 360. 10 mg of KL sample, after thorough dried under vacuum at 40 °C until, were dissolved in a 10 mL volumetric flask with 1,4-dioxane and the solution diluted to the mark with additional 1,4-dioxane. In the case of liquefied hydroxy-methylated KL, an aqueous solution of 10 mg (dry basis) was prepared in a 10 mL flask. Then, 1 mL of the resulting solution was transferred to three 25 mL volumetric flasks and each flask was filled to the mark with 0.2 N NaOH, pH 6 buffer solution, and pH 12 buffer solution. Gärtner-Gellerstedt method was then adopted (Gärtner et al. 1999). The absorbance of the 0.2 N NaOH and pH 12 alkaline solutions, recorder versus the pH 6 solution (ionization levels I and II, respectively) was measured in quintuplicate at 290–300 nm (Δa^{I}_{300}, Δa^{II}_{300}). Additionally, the absorbance of both solutions was recorded at 370 nm for KL, and 358–365 nm for hydroxy-methylated KL samples (Δa^{I}_{360}, Δa^{II}_{360}). The amount of the total *ph*-OH, the weakly acid C_5 substituted structures referred as "Condensed OH" phenolic structures, and the amount of free C_5 structures named as "G-OH" structures were estimated as follows:

$$\left[ph-\mathrm{OH}\right]\left(\mathrm{mmol\ g^{-1}}\right)=0.250\left(\Delta a^{II}_{300}\right)+0{,}107\left(\Delta a^{II}_{360}\right) \tag{1}$$

$$\left[\mathrm{Condesed\ OH}\right]\left(\mathrm{mmol\ g^{-1}}\right)=0.250\left(\Delta a^{II}_{300}-\Delta a^{I}_{300}\right)+0{,}107\left(\Delta a^{II}_{360}-\Delta a^{I}_{360}\right) \tag{2}$$

$$\left[\mathrm{G-OH}\right]\left(\mathrm{mmol\ g^{-1}}\right)=0.250\left(\Delta a^{I}_{300}\right)+0{,}107\left(\Delta a^{I}_{360}\right) \tag{3}$$

To discard a matrix interference due to the presence of unreacted reagents and potential undesirable products of *Cannizzaro* reaction the absorbance spectra of 0.1 N NaOH, 1 M F, 1 M formic acid, and 99.8 wt. % methanol solutions were analysed in the spectral range between 200 and 400 nm. Figure A1 (in Supplementary Material) depicts the overlap of the spectra of the four components, confirming the absence of the matrix absorption interferences within the *ph*-OH absorption range (300 and 360 nm).

Hydroxy-methylation increases the polarity of KL, possibly favouring self-assembly processes. To evaluate the impact of aggregation/disaggregation process on the reliability of the difference UV-method employing untreated liquefied samples (UL), the following sample pre-treatments were compared: vacuum-drying (VD), ultrasonication of the untreated liquefied samples (UL-US), and vacuum-drying followed by ultrasonication of the aqueous solution preparation (VD-US). Drying was performed under vacuum at 40 °C; ultrasonication was performed at room temperature at 40 kHz for 10 min.

Analysis of variance (ANOVA) of the response *ph*-OH variable at 95% confidence level was performed using a free version of the R software, 2023.06.1 Build 524 for Windows.

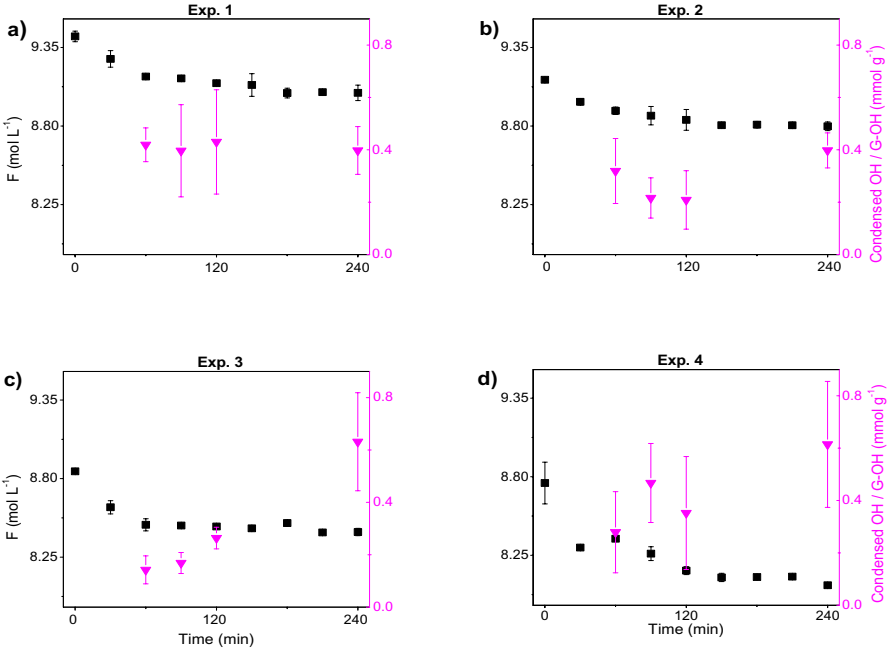

Fig. 1 Variation of [*F*] during reaction time (corrected by control reaction, mol g^{-1}) and the Condensed OH/G-OH ratio (mmol g^{-1}). **a** Exp. 1: pH 9 and 50 °C, **b** Exp. 2: pH 9 and 70 °C, **c** Exp. 3: pH 11 and 50 °C, and **d** Exp. 4: pH 11 and 70 °C

Gel permeation chromatography (GPC)

Method 1: 1 mg mL^{-1} sample solution in HPLC-grade DMSO was prepared by overnight stirring followed by filtration on 0.45 µm PFTE membrane. The filtrate was analysed with a Shimadzu HPLC equipped with a PKLel 5µm Mini-MIX-C, 250 × 4.6 mm; elution was performed with a 0.1 wt. % lithium chloride solution in HPLC-grade DMSO. The flow was set at 0.200 mL min^{-1} with an oven temperature of 70 °C. Molecular weights were determined by comparing the chromatograms with a calibration curve obtained with sulfonated polystyrene (246 – 2000000 g/mol) and low molecular weight lignin models.

Method 2: Molar mass distribution and averages were estimated using a Waters-Breeze Liquid Chromatograph. The chromatograph was equipped with a 1525 binary pump model with a Waters 717plus automatic injector. A set of (8×300mm) Shodex KD-802.5 columns was employed with a Waters 2414 model 410 differential refractive index detector. Dry samples were dissolved in 50 µL DMF with a final nominal concentration of 2 mg mL^{-1}. Before the injection, solutions were filtered through 0.45 µm PTFE filters. DMF was used as eluent with a flow rate of 1 mL min^{-1}; the oven of the chromatographer was set at 40 °C. Polyethylene glycol standards (PEG. Polymer Standards Service

GmbH (PSS). LOT: 10022015) were used for creating a calibration curve subsequently used for the analyses of the molecular weights.

Heteronuclear single quantum correlation (HSQC)

200 mg of sample were dissolved under stirring overnight at room temperature in 600 µL of a 1:1 (*v*/*v*) d^5-pyridine/ d^6-dimethylsulfoxide mixture; the resulting solution was analysed on an Avance 400 MHz Bruker NMR spectrometer; 16 scans were acquired obtaining a matrix consisting of 2048 × 2048 points (Crestini et al. 2011). Phase adjustment of the resulting spectra was performed using MestReNova.

^{31}P NMR analyses

^{31}P NMR analyses were performed according to the standard protocol reported by Granata and subsequent modifications (Argyropoulos et al. 2021; Granata & Argyropoulos 1995; Meng et al. 2019). 30 mg of accurately weighted and dried (40 °C, under vacuum, overnight) sample were dissolved in 500 µL of a 1.6:1 (*v*/*v*) pyridine/*d*-chloroform mixture plus 100 µL of internal standard (cholesterol) and relaxation agent (chromium (III) acetylacetonate) solution (in 1.6:1 (*v*/*v*) pyridine/*d*-chloroform mixture). After dissolution, the sample was phosphitylated with 100 µL of 1-chloro-4,4',5,5'-tetramethyl-1,3,2-dioxaphospholane; suddenly after, the spectrum of the resulting clear solution was acquired using a 300 MHz Bruker NMR spectrometer. Phase adjustment of the resulting spectra as well as integrations were performed using MestReNova.

Results and discussion

Free F and difference UV-analyses

The consumption of F at the end of the control reactions was between 1–2%. Figure 1 shows the variation in F concentration during the time, corrected by the F consumption of the control reactions, and the Condensed OH/G-OH ratio of the UL samples in KL hydroxy-methylation at different pH and temperature conditions.

The rate of consumption of F increased with the temperature and the pH. The consumption of F was respectively of 4.17%, 6.23%, 7.04%, and 10.35% at the end of hydroxy-methylations; the equilibrium concentrations were reached respectively after 180, 150, 60 and 150 min for Exp. 1–4. Further increase in reaction time did not result in an enhancement of F consumption, suggesting that the optimal time reactions were at the equilibrium. The Condensed OH/G-OH ratio remained almost constant for Exp. 1 at pH 9 and T = 50 °C, while a slight increase was observed only after 120 min when the hydroxy-methylation was performed at 70 °C. A marked incrementation of the Condensed OH/G-OH ratio was noticed when the reaction was performed at pH 11; a rapid increase in the consumption was achieved when the reaction was performed at 70 °C. Also, the final Condensed OH/G-OH ratio was higher for Exps. at pH 11 (≅ 0.6) than in the case of the reaction performed at pH 9

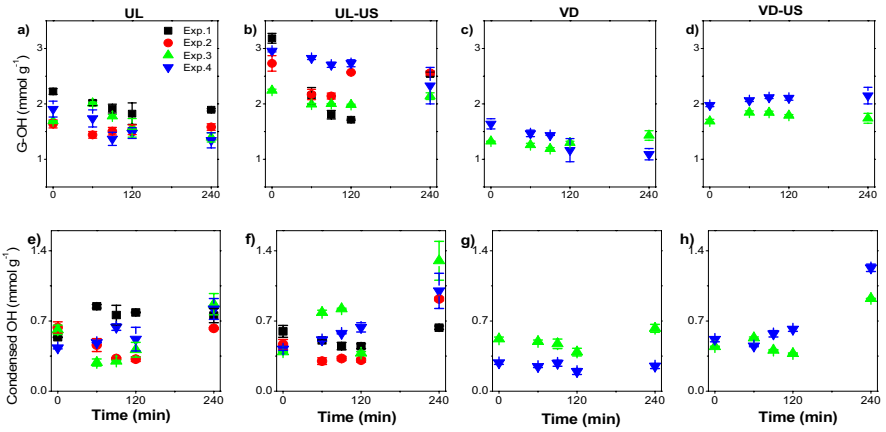

Fig. 2 Time evolution of G-OH and Condensed OH (mmol g^{-1}) for Exps. 1–4. UL, UL-US, VD and VD-US samples

at the same temperature (≅0.4). These experimental findings suggested the formation of new condensed structures from uncondensed guaiacyl units (Aini et al. 2019; Malutan et al. 2008).

The difference UV measurements (G-OH and Condensed OH) obtained from the different samples pre-treatments (UL, UL-US, VD, and VD-US) are compared in Fig. 2, while statistical analysis was performed for final *ph*-OH measurements (Table 2).

Despite all the liquefied samples were completely dissolved in water, vacuum dried samples synthesised at pH 9 (Exp. 1 and Exp. 2) resulted insoluble under UV-analyses conditions, consequently the method could not be applied in those cases. This result suggests that pH 9 is not alkaline enough to induce *ph*-OH ionization, repulsion, and dissolution of hydroxy-methylated KL molecules. This hypothesis is further supported by considering that the pK_a values for guaiacyl and syringyl units are slightly higher than 9.45. Instead, the propensity for aggregation is increased due to strong Van der Waals forces, π,π stacking and hydrogen bonding (Mishra & Ekielski 2019). Alkalinization of the final UL prepared at pH 9 to pH 11 prior to the vacuum drying process allowed the complete dissolution of the corresponding samples, named HKL1' and HKL2', due to *ph*-OH deprotonation.

As reported in Fig. 2, ultrasonication promoted a depolymerisation effect inducing an overestimation of G-OH (Gilca et al. 2015; Wells et al. 2013). This hypothesis was further supported by the higher values of UL-US and VD-US when compared to UL and VD, respectively. Additionally, an inversion in the consumption rate of the G-OH from Exp 1 to Exp. 4 occurred. The rate of G-OH consumption measured from UL [Fig. 2 a)] and VD [Fig. 2 c)] samples increased with temperature and pH (low rate for Exp. 1 and high rate for Exp. 4) in concordance with free F results (Fig. 1). Conversely, ultrasonicated samples showed the opposite effect, as the consumption rate increased from Exp. 4 to Exp. 1 [Fig. 2 b) and Fig. 2 d)]. Similarly,

Table 2 Final hydroxy-methylated KL: Total *ph*-OH of the untreated liquefied (UL), liquefied ultrasonicated (UL-US), vacuum-dried (VD), and vacuum-dried and ultrasonicated (VD-US) samples, using the difference UV-spectroscopic method

		HKL1	HKL2	HKL3	HKL4	HKL1'	HKL2'
ph-OH (mmol g^{-1})	UL	2.64 ± 0.06 [a]	2.26 ± 0.04[a]	2.27 ± 0.05[a]	2.16 ± 0.03[a]	2.90 ± 0.04[a]	2.35 ± 0.05[a]
	UL-US	3.21 ± 0.18[a]	2.60 ± 0.07[a]	3.51 ± 0.63[a]	3.32 ± 0.26[a]	3.29 ± 0.05[a]	2.83 ± 0.06[a]
	VD	—[b]	—[b]	2.04 ± 0.04	1.34 ± 0.14	2.76 ± 0.06	2.56 ± 0.04
	VD-US	—[b]	—[b]	2.65 ± 0.06	3.39 ± 0.37	2.72 ± 0.02	2.56 ± 0.05
Statistical comparison	*UL < UL-US*	*UL < UL-US*	*VD = UL* *UL < VD-US* *VD-US = UL-US*		*VD < UL* *UL < VD-US* *VD-US = UL-US*	*HKL1 = HKL1'*	*HKL2 = HKL2'*

[a] dry basis, and [b] not measured

an inversion in the formation rate of the Condensed OH was observed [Fig. 2 e) and Fig. 2 g) vs Fig. 2 f) and Fig. 2 h)].

The *ph*-OH variables were suitable for ANOVA model, as confirmed by assessing the assumptions of homoscedasticity (variance of the residuals is constant) and residuals normality (independent residues normally distributed with mean zero and variance for all factor levels). To explore significant differences among the samples a Tukey Test was employed.

As expected, ultrasonication leads to an overestimation of the total *ph*-OH. Regarding the vacuum-drying pre-treatment, no statistically significant differences between VD and UL were observed in HKL3. However, VD showed lower values compared to UL for HKL4. These findings suggest that the drying process of highly condensed samples could induce aggregation, making samples recalcitrant to disintegration leading to under-estimations (Agustin et al. 2019).

GPC analyses

Method 1

The GPC analyses revealed the molecular weight variations of KL deriving from the hydroxy-methylation under different conditions. The characterisation data are summarized in Table 3; the profile of the chromatograms is reported in Fig. 3.

The M_w of pristine KL was estimated as 1600 g mol^{-1}. In all cases, hydroxy-methylation resulted in an increase of the molecular weight of the starting material; this is evident from the chromatograms profile of hydroxy-methylated KL (Fig. 3), which clearly reveals the polymerisation by the intensification of the peak appearing at 15.7 min; the latter appeared as a minor shoulder of the major peak in the chromatogram of KL (maximum 16.7 min, Fig. 3). In all the hydroxy-methylated samples, the major peak of KL at 16.7 min, decreased in intensity becoming more and more a shoulder; this trend was especially evident for the profiles of HKL3 and HKL4.

In order to quantitatively determine the polymerising effect of the hydroxy-methylation on Eucalyptus KL, chromatograms were analysed using a calibration curve made of sulfonated polystyrene standards and low molecular weight lignin model compounds. In the case of HKL1, the M_w was estimated as 2600 g mol^{-1}, corresponding to almost the double of the starting material.

Table 3 Numeric (M_n) and ponderal (M_w) molecular weights with the corresponding dispersions ($Đ = M_w/M_n$) of KL and the hydroxy-methylated samples

	Method 1			Method 2		
	M_n	M_w	Đ	M_n	M_w	Đ
KL	700	1600	2.29	1865	22,925	12.29
HKL1	800	2600	3.25	2900	26,100	8.88
HKL2	900	2900	3.22	3000	27,400	9.19
HKL3	1000	3800	3.80	4900	33,000	6.73
HKL4	1000	4000	4.00	6000	34,700	5.83

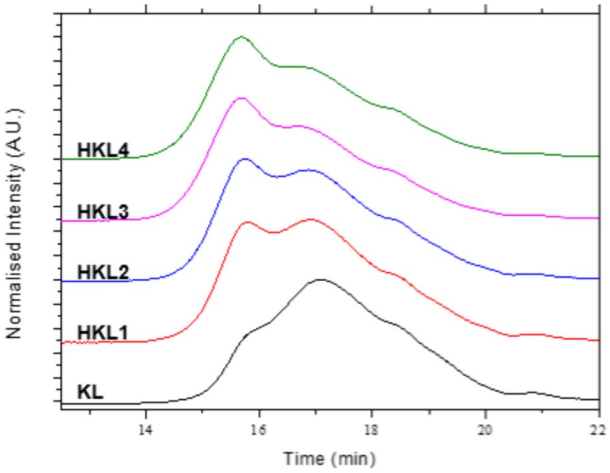

Fig. 3 Chromatograms for KL and the hydroxy-methylated samples

The variation of reaction parameters such as the temperature and the pH, affected to different extents the M_w of the hydroxy-methylated sample. From one side, the increase of the temperature, HKL2, resulted in an increase of the M_w, which became of 2900 g mol^{-1}. From the other side, a more efficient effect on the M_w was achieved under stronger alkaline reaction conditions; in fact, the reaction performed at pH 11, HKL3, exhibited a more than two-folded increase in the M_w (3800 g mol^{-1}).

The synergistic beneficial effect of both parameters on the M_w was revealed in the case of HKL4; in fact, by performing the reaction at 70 °C at pH 11, gave the highest M_w of the series, corresponding to 4000 g mol^{-1}.

Method 2

Figure 4 shows the chromatograms of KL [Fig. 4a)] and hydroxy-methylated KL [Fig. 4b)-e)], meanwhile average data are in Table 3. The results align with the standard protocol. The profiles are much better resolved but showed a slightly higher molecular weight due to the different calibrations.

Differently from Method 1, Method 2 allowed to determine the percentage composition of the various fractions characterising hydroxy-methylated samples, after the deconvolution of chromatograms with a routine implemented in Matlab. This routine employed an exponentially modified Gaussian function to fit each peak individually (Clementi et al. 2015). The curve deriving from the sum of individual peaks closely replicates the chromatograms observed for the examined samples. The percentage proportion of oligomers present in each sample was calculated based on the area of each distinct peak and the overall area of the corresponding chromatogram. Additionally, for every peak, the associated molar mass was estimated utilizing the direct calibration method. The results, summarized in Table 3, confirm the polymerisation of KL along hydroxy-methylation. Higher molecular weight fractions increased with temperature

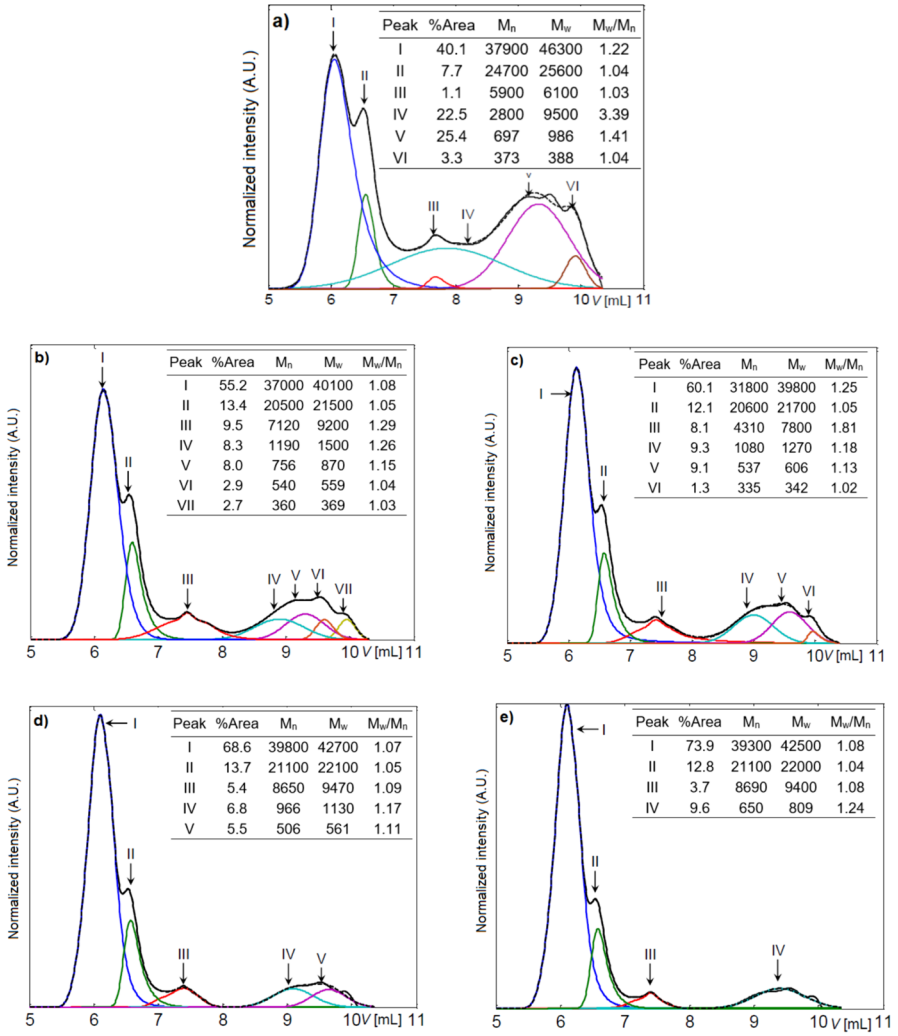

Fig. 4 Chromatograms deconvolution for: **a** KL, and final hydroxy-methylated lignins: **b** HKL1 (pH 9, 50 °C), **c** HKL2 (pH 9, 70 °C), **d** HKL3 (pH 11, 50 °C), and **e** HKL4 (pH 11, 70 °C)

and pH, at the expense of the lower molecular weight fractions. However, the impact of pH was higher at the same temperature. These results aligned with those obtained with Method 1. The application of the deconvolution routine permitted to discern the various contributions of each polymeric fraction to the overall polymeric material, which was considered as a "whole" material by Method 1.

Considering the results for F time consumption (Fig. 1) the following mass-balance can be written:

$$[\mathrm{F}]^0 = [F] + \left[-CH_2OH\right] + \left[-CH_2-\right] \tag{4}$$

where $[F]^0$ is the total initial F (Table 1). In the absence of condensation, *Eq.* 4 reduces to:$[F]^0 = [F] + \left[-CH_2OH\right]$; and equilibrium is reached due to the reversibility of hydroxy-methyation reactions. In the presence of condensation, $\left[-CH_2-\right]$ increases at the expense of $\left[-CH_2OH\right]$.

By assuming condensation processes as negligible, a gross and indirect estimation of the average molar mass of hydroxy-methylated KL can be obtained according to:

$$M_n = \frac{M_{LK}\left[KL^0 + M_F\left([F]^0 - [F]\right)\right]}{KL^0} \quad (5)$$

where KL^0 is the initial concentration of KL in g L^{-1} (Table 1) and $([F]^0 - [F])$ represents the concentration of consumed F. M_{LK} and M_F (= 30 g mol^{-1}) represent the molar masses of the pristine KL and F, respectively. According to GPC results, M_{Lk} is 700 g mol^{-1} for Method 1 and 1865 g mol^{-1} for Method 2. Thus, the M_n for HKL1, the less condensed hydroxy-methylated KL, is 729 g mol^{-1} and 1942 g mol^{-1} from *Eq.* 5, respectively. Despite the gross assumption of the lack of condensation, the corresponding error for Method 1 and Method 2 is 8.9% and 33%. We can conclude that Method 1 exhibits higher accuracy for lignin derivatives, whereas Method 2 may be more suitable for separating higher lignin-phenol adducts in resol synthesis.

HSQC analyses

In order to understand how KL is hydroxy-methylated, the HSQC spectra of KL and the hydroxy-methylated HKL1, HKL2, HKL3, and HKL4 were acquired in the d^5-pyridine/d^6-dimethylsulfoxide mixture described by Kim (Kim & Ralph 2010). The full spectra are reported in Fig. 5.

From Fig. 5a–e it is evident that in no case signals deriving from the degradation-products of F by *Cannizzaro* reaction were revealed (formic acid or its sodium salt, sodium formiate, signals around 170 ppm at ^{13}C); this fact is in agreement with reported formic acid formation obtained only when high alkalinity is coupled with elevated temperatures (Yang et al. 2015).

The characteristic regions for the HSQC spectra of KL and hydroxy-methylated samples were compared to elucidate the sites as well as the degree of functionalization of the starting materials. The signals appearing in the oxygenated and aromatic areas were, in this perspective, especially useful. Semi-quantitative analyses of the most relevant signals appearing in these ranges was performed according to standard procedures (Crestini et al. 2011; Sette et al. 2011). The data are reported in Table 4 and Table 5.

Aliphatic region. The aliphatic region of the spectra displays various signals characterised by similar correlation peaks. In particular, not only the C/H cross-correlation peaks of KL impurities (such as wood-extractives like fatty acids, turpentine, and exudates), stylbene signals appeared (Crestini et al. 2017), but also those

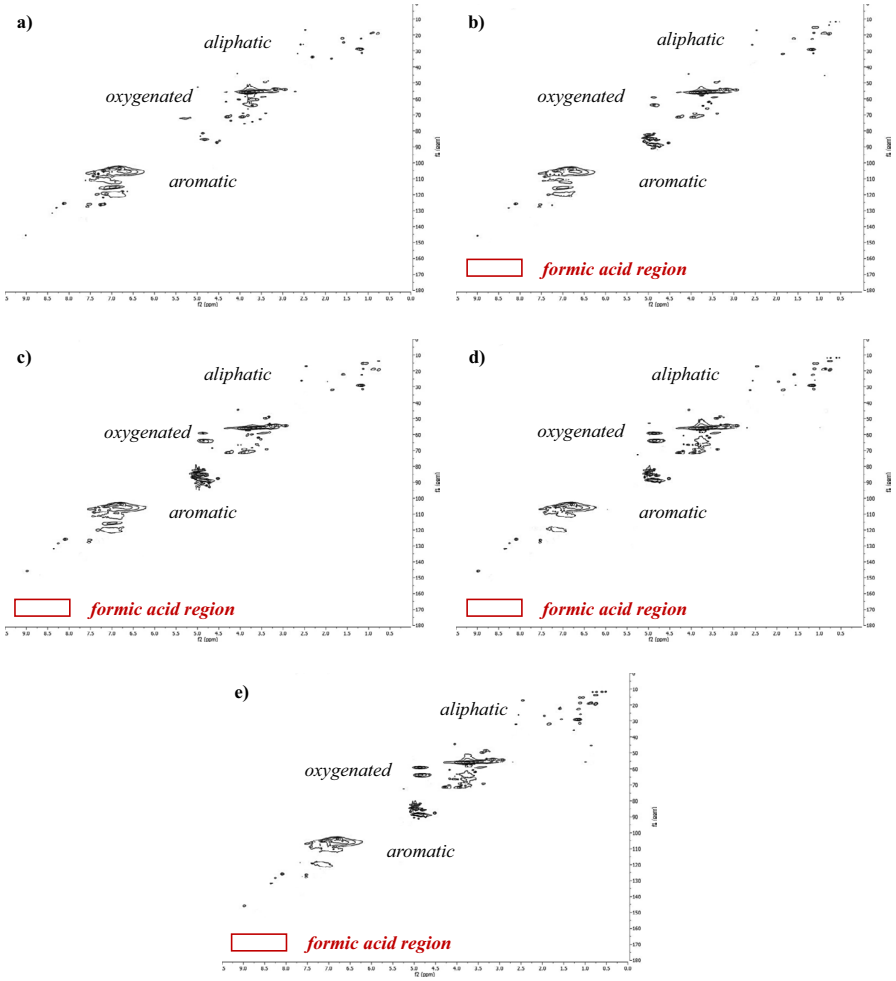

Fig. 5 Total HSQC 2D spectra, δC/δH 0–185/0.0–9.5 ppm: **a** pristine KL, **b** HKL1, **c** HKL2, **d** HKL3, and **e** HKL4. The characteristic region for formic acids cross-signal is highlighted

Table 4 Content of the aliphatic carbons constituting the aliphatic domains in the most abundant bonding-patterns of KL and the hydroxy-methylation products. Contents are expressed on the basis of 100 phenyl-propanoic units

	A_α	A_β	A_γ	B_α	B_β	B_γ	M_1	M_2	N	K_α
KL	2.50	0.90	0.40	3.30	4.20	1.70	0.00	0.00	0.00	0.90
HKL1	0.90	0.90	0.90	1.80	6.30	3.60	0.90	1.80	2.70	0.00
HKL2	0	0.90	1.40	1.80	6.30	2.70	0.90	3.60	3.60	0.90
HKL3	0	1.00	1.00	3.80	8.680	3.80	4.30	4.80	4.30	1.00
HKL4	0	0.90	0.90	3.50	7.00	3.50	4.00	4.40	4.60	0.90

Table 5 Syringyl ($S_{2,6}$)/guaiacyl (G_2) ratios (S/G) and content of G_2, G_5 and G_6 units, based on 100 phenyl-propanoidic units, of KL and hydroxy-methylated samples

	S/G	$S_{2.6}$	G_2	G_5	G_6
KL	3.30	86.70	13.30	15.00	13.30
HKL1	4.10	89.20	10.80	9.90	10.80
HKL2	4.20	89.30	10.70	6.30	10.70
HKL3	5.30	91.40	8.60	0.00	7.60
HKL4	5.20	91.20	8.80	0.00	7.90

pertaining to the methylene-bridges formed during hydroxy-methylation-induced ring-condensation (more details on them are reported in the upcoming paragraphs).

Oxygenated region. The oxygenated area of the HSQC spectrum of KL [Fig. 6a] reveals the typical cross-signals for the aliphatic C-H couplings of KL; *methoxy* ((*-OMe*)55.8/3.80 ppm), *aryl-glycerol-β-aryl* ((*A*)72.3/5.29, 87.7/4.33, and 58.7/3.44 ppm), and *resinol* ((*B*)85.4/4.84, 54.1/3.20, and 71.2/4.30–71.2/3.95 ppm) (Ibarra et al. 2007). These signals were also prominent in the hydroxy-methylated samples [Fig. 6b–e].

Comparing the oxygenated area of the HSQC spectrum of pristine KL and the hydroxy-methylated sample allowed speculations on the mechanism of KL hydroxy-methylation. In particular, it was concluded that under the reaction conditions, hydroxy-methylation followed the *Lederer—Manasse* mechanism leading to the introduction of methylol groups onto the aromatic ring. This was supported by the appearance of two strong signals at 59.1/4.87 and 63.8/4.86 ppm [M in Fig. 6 b)-e)], undetected on the starting KL, which were assigned to the methylol groups at the C_5 position of guaiacyl units (—CH_2OH) (Paananen & Pakkanen 2020; Zhao et al. 1994). The duplication of the signal was attributed to the hydroxy-methylation respectively of guaiacyl-glycerol-β-aryl ether (A) and resinol (B) patterns.

The presence of C_α carbonyls in KL in certain syringyl units ($S_{2,6}$') suggested the potential addition of methylols in β-position of the propanoidic chain, according to the Tollens mechanism. However, this hypothesis was excluded due to the absence of the corresponding signals around 70–72 ppm observed by Paananen (Paananen & Pakkanen 2020).

Not only the methylol groups were added to KL during hydroxy-methylation. In fact, the signal at 88.8/4.86 ppm was attributed to addition product of dimethylene-glycol to lignin [—CH_2-O-CH_2-OH, N, which appears in Fig. 6 b)-e)] (Peng et al. 1992).

The other cross-peaks at 82.5/4.90 and 86.6/5.10 ppm were assigned to by-products deriving from the acetalization of F in alkaline conditions and its dimerization product (Rivlin et al. 2015), methylene-glycol and free di-methylene-glycol respectively.

Semi-quantitative HSQC analyses of the oxygnenated area (Table 4) allowed the quantification of the transformation previously described. Specifically, the content of methylol groups onto the guaiacyl units (M) increased from HKL1 to HKL4, supporting the results obtained by estimating F consumption, which revealed the beneficial effect of the pH and the temperature on the reaction. In fact, by performing

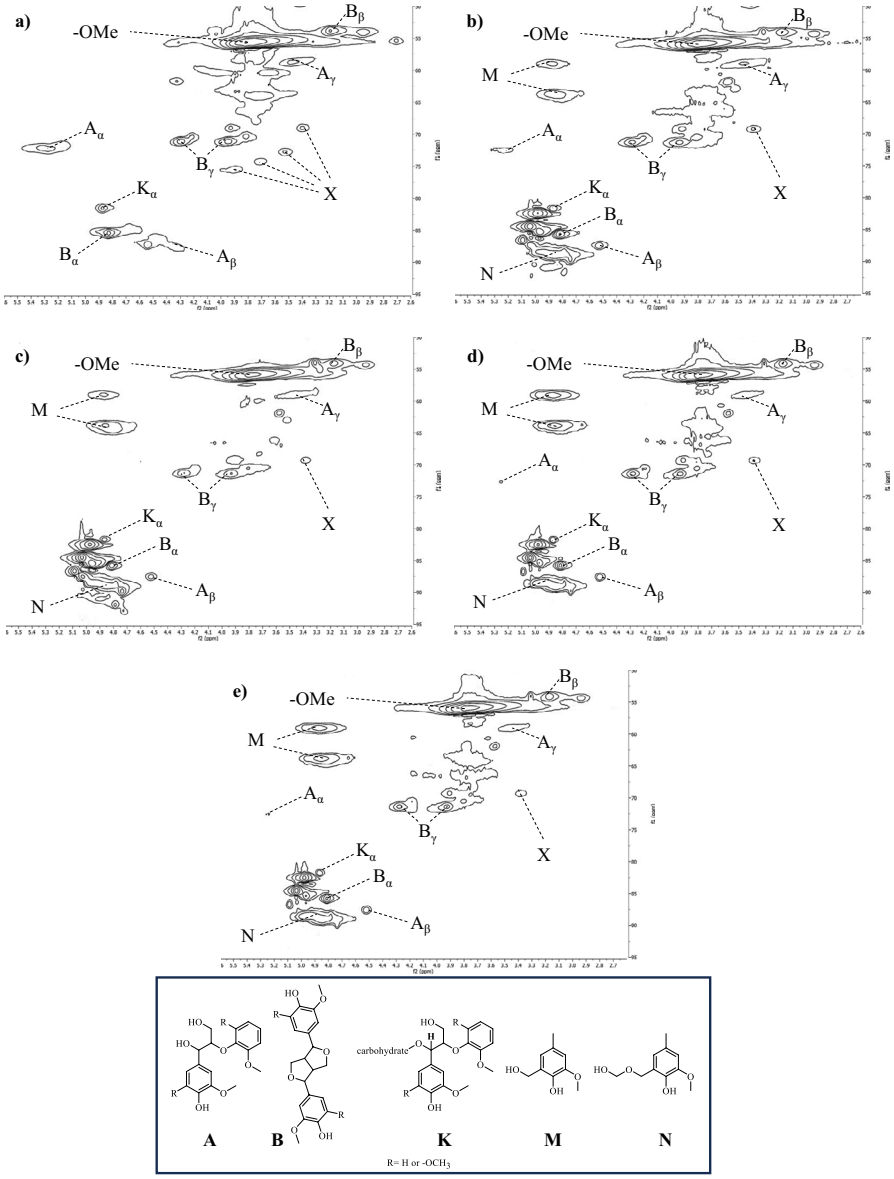

Fig. 6 Oxygenated area of the HSQC 2D spectra, δC/δH 50–95/2.5–5.6 ppm: **a** pristine KL, **b** HKL1, **c** HKL2, **d** HKL3, and **e** HKL4

hydroxy-methylation at 50 °C it was noticed that an increase in pH (HKL1, pH 9 and HKL3, pH 11) resulted in a relevant incrementation in the addition of hydroxymethyl groups onto the guaiacyl units; in fact, the amount of M was the highest of the series under these conditions. The simultaneous increase in N was attributed to the alkalinity effect on the dimerization of F; as the pH raises, the formation of

dimethylene-glycol is favoured leading to an increased degree of functionalization with this species.

A relatively beneficial effect of temperature on the degree of hydroxy-methylation was revealed by increasing the temperature to 70 °C, as reported in the case of HKL2; under these conditions, an increase in the amount of M was noticed, if compared to HKL1. Conversely, although the contemporary increase in pH and temperature (HKL4, pH 11 and 70 °C) resulted in an enhancement in F consumption, it had a negative effect on hydroxy-methylation. HKL4 revealed a lower content in M and a higher content in N (the glycol-derivative side product) than HKL3; this fact was in line with the effect of alkalinity on the formation of F dimerization products.

In conjunction with the increase in hydroxy-methylation, a decrease in the content of A_α was observed, suggesting the participation of benzylic carbon of aryl-glycerol-β-aryl on hydroxy-methylation. This phenomenon, previously observed and reported by Paananen (Paananen & Pakkanen 2020) will be envisaged in future investigations.

Aromatic region. The aromatic area of KL HSQC spectrum (Fig. 7) not only revealed the presence of *syringyl* ($S_{2,6}$ 104.7/6.91), and *guaiacyl* (G_2 111.9/6.91, G_5 115.6/6.98, and G_6 119.4/6.95 ppm) units, but also demonstrated the presence of syringyl units bearing a carbonyl in α-position on the propanoidic side chain, indicated by the weak correlation peak at 106.2/7.38 ppm. The same type of signals was revealed also in the case of hydroxy-methylated samples [Fig. 7 b)—e)]. The comparison of the spectra demonstrated the selectivity of the methylol addition to the C_5 position of guaiacyl-units as evidenced by the progressive disappearance of the correlation C/H signal going from Fig. 7 b) to Fig. 7 e). Semi-quantitation of these functional groups confirmed this hypothesis (Table 5). These findings align with the methylol signals in the oxygenated region.

Not only G_5 signals varied in intensity; G_2 and G_6 content also decreased in hydroxy-methylated samples if compared to the starting pristine lignin. This variation was attributed to the generation of new condensed structures, where guaiacyl units were bond together via a methylene substituent on G_5. Therefore, it was hypothesized that the condensation of guaiacyl units affected the chemical shifts of G_2 and G_6, shifting them to values like those of S_2 and S_6 due to their structural similarity. This hypothesis was confirmed by the evident incrementation in the S/G ratio observed (from 3.30 in KL to 5.20 in HKL4) deriving from the intensification of $S_{2,6}$ signals.

The observed lack in reactivity of syringyl units was supported by early studies of Marton describing the higher reactivity of guaiacyl units (Marton et al. 1966).

^{31}P NMR

^{31}P NMR analyses allowed the quantification of hydroxylated moieties as well as their differentiation into aliphatic, terminal phenolic, and carboxylic. The comparison of the spectra of P-labelled KL with the hydroxy-methylation products

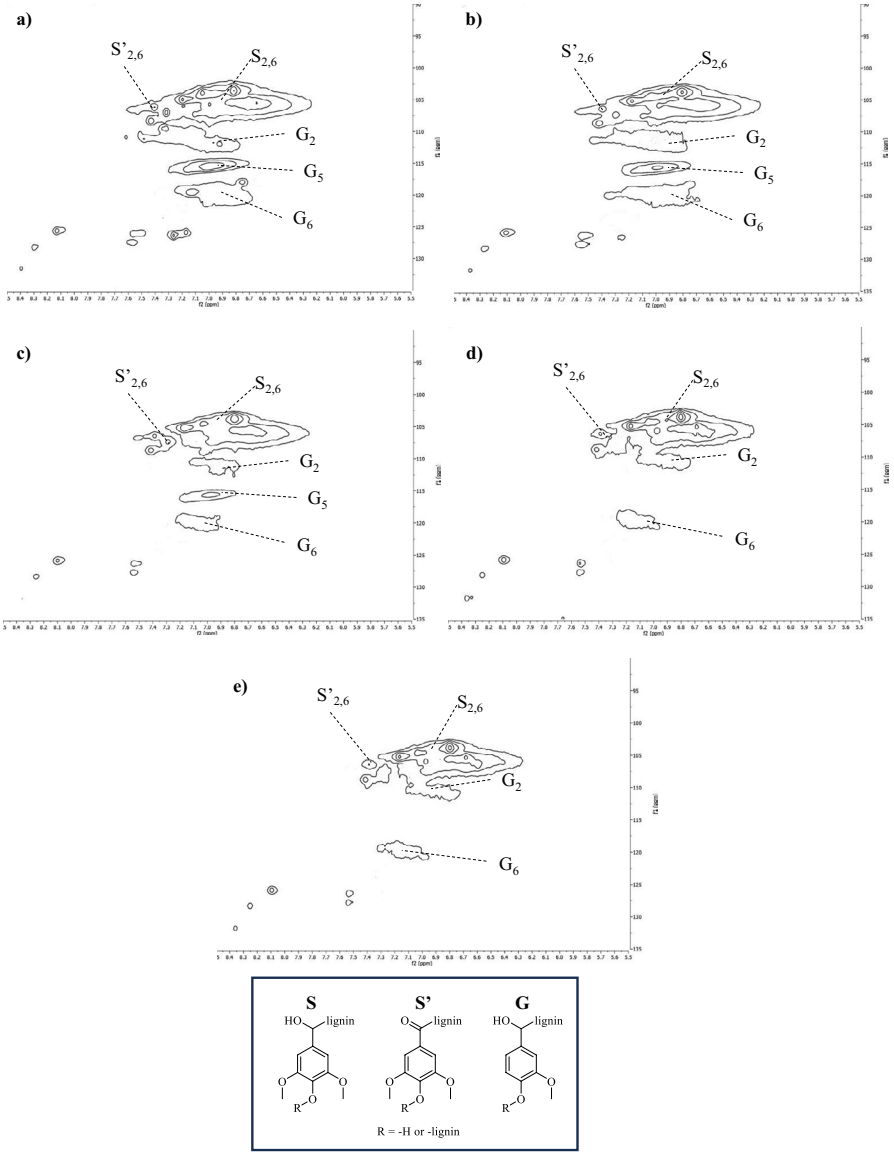

Fig. 7 Aromatic area of the HSQC 2D spectra, δC/δH 90–135/5.5–8.5 ppm: **a** pristine KL, **b** HKL1, **c** HKL2, **d** HKL3, and **e** HKL4

is reported in Fig. 8. The quantitation of the functional groups is summarized in Table 6.

An accurate quantification of aliphatic hydroxyl groups was not possible due to the residual traces of F acetalization and dimerization products; this was revealed by the presence of strong spikes in the range between 149–146 pp, which did not appear in KL. In particular, the methylene glycol and di-methylene glycol impurities

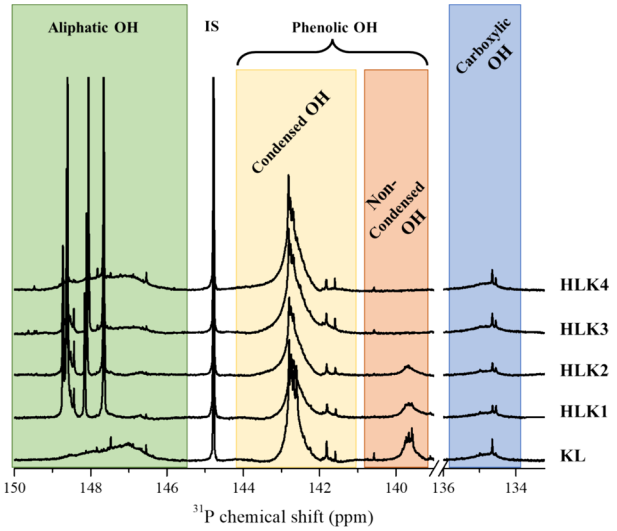

Fig. 8 ^{31}P NMR spectra and corresponding assignments for KL and hydroxy-methylated KLs after phosphitylation with 1-chloro-4,4',5,5'-tetramethyl-1,3,2-dioxaphospholane. IS signal pertain to the derivatised internal standard utilised for the quantitative analyses

Table 6 Content of the hydroxylated moieties involved in the hydroxy-methylation of KL estimated via ^{31}P NMR

	Aliphatic OH (mmol g^{-1})	Condensed OH (mmol g^{-1})	Guaiacyl OH (mmol g^{-1})
KL	0.89	0.48	0.33
HKL1	1.61	0.49	0.31
HKL2	1.21	0.59	0.09
HKL3	0.85	0.60	0.00
HKL4	1.00	0.62	0.00

already revealed in the HSQC spectra, exhibited strong signals around 149 ppm, when P-labelled, according to Li et al. (2018). In the same chemical shift range, also two intense peaks appeared at 148.2 and 147.8 ppm; the latest were attributed to the methylol and di-methylene-glycol-free bound to the C_5 in guaiacyl units. Their content was not quantified to avoid over- or under-estimation due to the unnegligible overlapping with other aliphatic hydroxyl-groups already present in KL.

If HSQC spectra revealed that the favoured products of KL hydroxy-methylation are those in charge of guaiacyl units according to the *Lederer-Manasse* mechanism, the ^{31}P NMR quantitation of phenolic moieties permitted to unequivocally identify the optimum conditions for the complete hydroxy-methylation of terminal G_5. With this respect, the content of condensed (syringyl, 4-O-5', and 5,5' units) and guaiacyl units played a fundamental role. The plot of their content in KL and hydroxy-methylation products obtained under different conditions is depicted in Fig. 9.

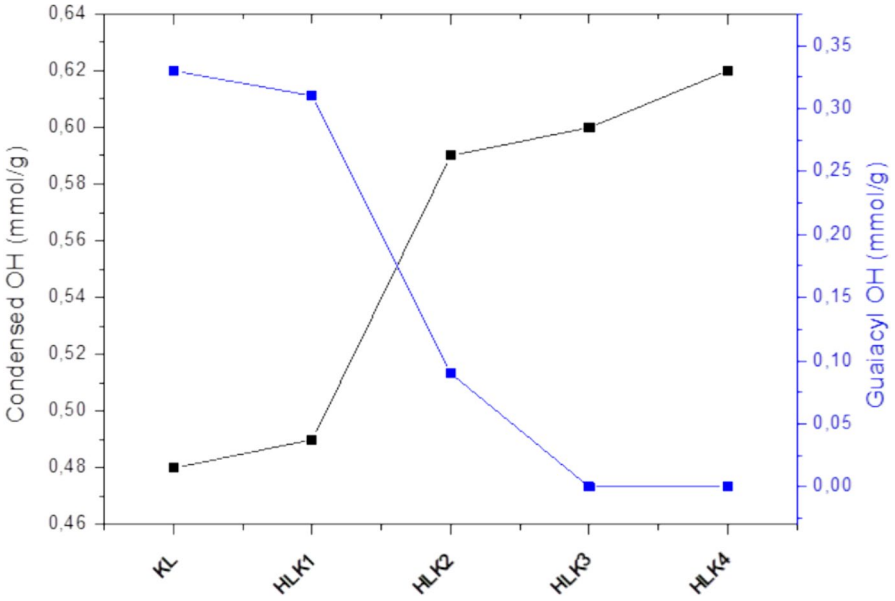

Fig. 9 Content of condensed (syringyl, 4-O-5', and 5,5') and guaiacyl units in KL and its hydroxy-methylation products

An evident decreasing trend in guaiacyl units was revealed going from HKL1 to HKL4, where they fully disappear in HKL3 and HKL4. On the opposite, the content of condensed units proportionally increases. These experimental findings were attributed to the formation of diaryl-methane (5-CH_2-5', Scheme 1) patterns; in fact, methylene-linked guaiacyl-units chemical shift coincides to condensed structures, which are characterised by a different chemical shift of unmodified terminal guaiacyl (140.2–138.8 ppm).

Spectral simulations permitted to calculate the chemical shifts of the correlation peak of the methylene bridge between aromatic rings; in fact, it should appear in the aliphatic region of the HSQC spectra ($\delta_C \sim 29.6$ ppm and $\delta_H \sim 4.98$ ppm). However, due to the complexity of this spectral region, it was not feasible to unequivocally assign the present signal in the spectra of HKL1, HKL2, HKL3, and HKL4.

These results obtained via ^{31}P NMR confirmed those previously obtained via the difference-UV method, suggesting an increase in the degree of condensation of

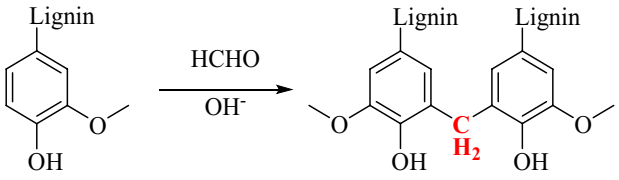

Scheme 1 Formation of condensation product of terminal guaiacyl units via F addition and condensation

lignin samples during hydroxy-methylation, especially while performing the reaction at pH 11.

In fact, it was concluded that the full hydroxy-methylation of KL can be obtained at pH 11 either at 50 (HKL3) or 70 °C (HKL4). Due to the intrinsic error in ^{31}P NMR analyses, estimated in the present analyses as around 8%, the different content in condensed units between HKL3 and HKL4 (0.02 mmol g^{-1}) can be considered negligeable. The coupling of HSQC data (demonstrating the complete disappearance of G_5 in HKL3 and HKL4 with the contemporary increase in M signal intensity) with these quantitative data (revealing the complete disappearance of terminal guaiacyl units in HKL3 and HKL4) allowed to conclude that, if side-reactions yielding the formation of dimethylene-glycol addition products are excluded, the optimum reaction conditions for the hydroxy-methylation of KL are pH 11 and 50 °C (HKL3). These results align with the temperature previously identified by Zhao for softwood KL (Zhao et al. 1994); moreover, the lower alkalinity (pH 11, present work; pH 12, Zhao et al. 1994) and the shorter reaction time (1 h, present work; 2 h, Zhao et al. 1994) identified in the present work as the optimal condition suggest a different reactivity. These differences were attributed to the presence of syringyl units, imparting a different behaviour to the material. Additionally, the estimation of S/G ratio, according to the ratio of terminal phenolated moieties ^{31}P NMR data, revealed an increase with the intensification of the reaction conditions, as already demonstrated in the HSQC analyses.

Finally, the analyses of spectral range of 136.0–134.0 ppm, corresponding to P-labelled carboxylic moieties revealed that no new acidic centres were formed during hydroxy-methylation, as their content remains almost the same from KL and the hydroxy-methylated samples. Additionally, this finding supports the lack of residual traces of F by-products (formic acid), formed via *Cannizzaro* reaction, already postulated on evaluating the HSQC spectra.

On the Eucalyptus KL hydroxy-methylation mechanism

Terminal phenolic moieties of KL behave in the same manner of phenol under alkaline hydroxy-methylation (Scheme 2), generating either diaryl-methane or the M and N adducts depicted in Fig. 6. The only difference from phenol is represented by the locked *p*-position with respect to the hydroxyl group by the lignin aliphatic chain.

^{31}P NMR analyses supported the UV–vis analyses results to identify the optimum conditions for the full functionalization of terminal phenolated moieties. Moreover, both techniques could not provide quantitative information on the transformations occurred on the internal aromatic moieties during hydroxy-methylation, as both rely on free-phenols measurements. On the contrary, HSQC analyses revealed the complete disappearance of G_5 signals (either internal or terminal) as the reaction proceeded under different conditions. This fact, coupled with the observed increment in the S/G ration, suggested the participation of internal guaiacyl units in the hydroxy-methylation. Considering the activating nature of alkoxy- substituents onto

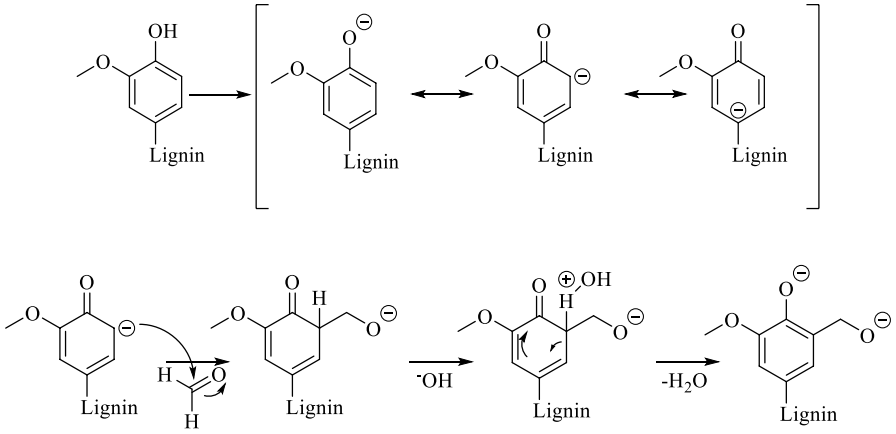

Scheme 2 Eucalyptus KL hydroxy-methylation

the internal guaiacyl units, which results in the supply of electrons via M + mesomeric effect on the aromatic ring, Scheme 3 could be hypothesised..

The dislocation of valence electrons of ethereal oxygen forms an oxonium specie and a carbanion on G_5. The latest can easily undergo F addition according to the mechanism depicted in Scheme 3. Once the condensation product is formed, the elimination of the G_5 proton mediated by the alkaline environment repristinate a negative charge which displaces on the ring favouring the re-aromatisation of the system. At the same time, the double bond at the base of oxonium cation is neutralized repristinating the single bond. According to this mechanism, it was possible to fully rationalize the transformations occurred under the different reaction conditions. Further experimental work will be performed in order to confirm the present hypothesis.

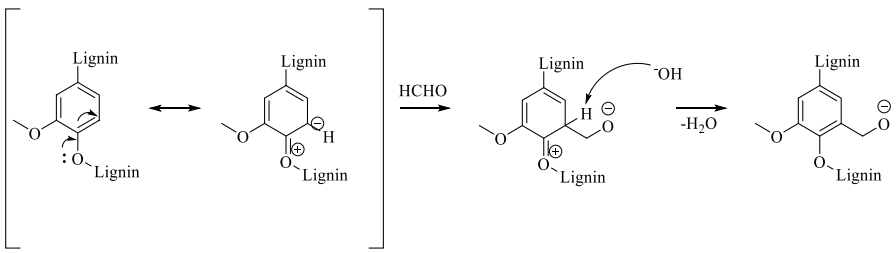

Scheme 3 Activation of internal guaiacyl units during hydroxy-methylation

Conclusion

In the present work the hydroxy-methylation of Eucalyptus KL was investigated under different temperature and pH conditions, demonstrating the complete hydroxy-methylation under pH condition of 11 and at 50 °C and 70 °C. Strong alkalinity promoted an increase of the average molecular weights, of the uptake of F and of the Condensed OH/G-OH ratio, which was attributed to the condensation of C5 guaiacyl units via methylene bonds. Furthermore, the formation of dimethylene-glycol addition products was favoured under these conditions, especially at 70 °C.

The molecular weight profiles obtained by GPC using a Shodex KD 802.5 columns with DMF as eluent exhibited a higher resolution if compared to those obtained using the PLGel MiniMIX-C column with DMSO. This strategy, coupled with a rigorous deconvolution approach, permitted to better identify the oligomeric species deriving from KL hydroxy-methylation. However, the role of the calibration was found to be crucial; in fact, the use of a calibration curve made of sulfonated polystyrene standards and lignin models provided a more accurate estimation of the average molecular weights for the hydroxy-methylated KL than PEG standards.

The increase in the Condensed OH/G-OH ratio was confirmed via difference UV-spectroscopic method, as well as the ^{31}P NMR and ^{1}H–^{13}C HSQC NMR techniques.

Of the three analytical techniques employed, the aqueous difference UV-spectroscopic method allowed an in-flow monitoring of the Condensed OH/G-OH ratio, permitting to study the kinetic of the reaction. This is especially pertinent as ultrasonication and vacuum-drying encourage depolymerisation and self-assembly of the KL samples, potentially resulting in over-estimations and under-estimations, respectively.

The optimal reaction conditions for the hydroxy-methylation of KL, excluding side-reactions leading to the formation of dimethylene-glycol addition products, are pH 11 and 50 °C for a period time of one hour, reaching equilibrium.

The selectivity of the *Lederer-Manasse* reaction, highlighted by the absence of undesirable *Cannizzaro* products and the lack of formation of hydroxymethyl groups in the aliphatic chain, makes Eucalyptus KL an encouraging source for the synthesis of resols.

Supplementary Information The online version contains supplementary material available at https://doi.org/10.1007/s00226-024-01596-5.

Acknowledgements This research was financially supported by Agencia I+D+i (Grant. No 2019-2019-04193), Universidad Tecnológica Nacional (Grant No. PID MAUTISF0007635TC and PID PATCBS-F0008135TC), and CONICET (Grant. No GI 11220200101041CO) from Argentina, and Consorzio Interuniversitario per lo sviluppo dei Sistemi a Grande Interfase (Center for Colloid and Surface Science) from Italy.

Author contributions M.P. and N.P. carried out the experimental work and wrote the main manuscript text. C.C. and V. N. supervised the project. All authors reviewed the manuscript.

Funding Center for Colloid and Surface Science,Agencia Nacional de Promoción Científica y Tecnológica,2019-04193,Universidad Tecnológica Nacional, MAUTISF0007635TC, Consejo Nacional de Investigaciones Científicas y Técnicas, GI 11220200101041CO.

Data availability No datasets were generated or analysed during the current study.

Declarations

Conflict of interest The authors declare no competing interests.

References

Agustin MB, Penttilä PA, Lahtinen M, Mikkonen KS (2019) Rapid and direct preparation of lignin nanoparticles from alkaline pulping liquor by mild ultrasonication. ACS Sustain Chem Eng 7(24):19925–19934. https://doi.org/10.1021/acssuschemeng.9b05445

Aini NAM, Othman N, Hussin MH, Sahakaro K (2019) Hydroxy-methylation-modified lignin and its effectiveness as a filler in rubber composites. Processes 7:315–336. https://doi.org/10.3390/pr7050315

Alonso MV et al (2001) Characterization and structural modification of ammonic lignosulfonate by methylolation. J Appl Polym Sci 82(11):2661–2668. https://doi.org/10.1002/app.2119

Argyropoulos DS, Pajer N, Crestini C (2021) Quantitative 31P NMR analysis of lignins and tannins. JoVE 174:1–21. https://doi.org/10.3791/62696

Argyropoulos DS, Crestini C, Dahlstrand C et al (2023) Kraft Lignin: A Valuable, Sustainable Resource. Oppor Chall Chemsuschem 16(23):1–34. https://doi.org/10.1002/cssc.202300492

Campbell AG, Walsh AR (1985) The present status and potential of kraft lignin-phenol-formaldehyde wood adhesives. J Adhesion 18(4):301–314. https://doi.org/10.1080/00218468508080465

Chen Y, Zhang H, Zhu Z, Fu S (2020) High-value utilization of hydroxy-methylated lignin in polyurethane adhesives. Int J Biol Macromol 152:775–785. https://doi.org/10.1016/j.ijbiomac.2020.02.321

Clementi LA, Meira GR, Berek D, Ronco LI, Vega JR (2015) Molar mass distributions in homopolymer blends from multimodal chromatograms obtained by Sec/Gpc with a concentration detector. Polym Test 43:58–67. https://doi.org/10.1016/j.polymertesting.2015.02.007

Crestini C, Melone F, Sette M, Saladino R (2011) Milled wood lignin: a linear oligomer. Biomacromol 12(11):3928–3935. https://doi.org/10.1021/bm200948r

Crestini C, Lange H, Sette M, Argyropoulos DS (2017) On the structure of softwood kraft lignin. Green Chem 19(17):4104–4121. https://doi.org/10.1039/c7gc01812f

Dilling P (1987) Method for methylolation of lignin materials. U.S. Patent 4,764,597, 19:1–5. Available at: https://patents.google.com/patent/US4764597A/en?q=methylolation&q=lignin&oq=methylolation+lignin.

Eliav MU, Navon G (2015) NMR studies of the equilibria and reaction rates in aqueous solutions of formaldehyde. J Phys Chem B 119(12):4479–4487. https://doi.org/10.1021/jp513020y

El Mansouri NE, Yuan Q, Huang F (2011) Synthesis and characterization of kraft lignin-based epoxy resins. BioResources 6(3):2492–2503. https://doi.org/10.15376/biores.6.3.2492-2503

El Mansouri NE, Qiaolong Y, Farong H (2018) Preparation and characterization of phenol-formaldehyde resins modified with alkaline rice straw lignin. BioResources 13(4):8061–8075. https://doi.org/10.15376/biores.13.4.8061-8075

Gärtner A, Gellerstedt G, Tamminen T (1999) Determination of phenolic hydroxyl groups in residual lignin using a modified UV-method. Nord Pulp Pap Res J 14(2):163–170. https://doi.org/10.3183/npprj-1999-14-02-p163-170

Gilca IA, Popa VI, Crestini C (2015) Obtaining lignin nanoparticles by sonication. Ultrason Sonochem 23:369–375. https://doi.org/10.1016/j.ultsonch.2014.08.021

Granata A, Argyropoulos DS (1995) 2-Chloro-4,4,5,5-tetramethyl-1,3,2-dioxaphospholane, a reagent for the accurate determination of the uncondensed and condensed phenolic moieties in lignins. J Agric Food Chem 43(6):1538–1544. https://doi.org/10.1021/jf00054a023

Ibarra D, Chávez MI, Rencoret J et al (2007) Lignin modification during Eucalyptus globulus kraft pulping followed by totally chlorine-free bleaching: a two-dimensional nuclear magnetic resonance, Fourier transform infrared, and pyrolysis-gas chromatography/mass spectrometry study. J Agric Food Chem 55(9):3477–3490. https://doi.org/10.1021/jf063728t

Kim H, Ralph J (2010) Solution-state 2D NMR of ball-milled plant cell wall gels in DMSO-d 6/pyridine-d5. Org Biomol Chem 8(3):576–591. https://doi.org/10.1039/b916070a

Kun D, Pukánszky B (2017) Polymer/lignin blends: interactions, properties, applications. Eur Polym J 93:618–641. https://doi.org/10.1016/j.eurpolymj.2017.04.035

Kuo M, Hse CY, Huang DH (1991) Alkali treated kraft lignin as a component in flakeboard resin. Holzforschung 45:47–54. https://doi.org/10.1515/hfsg.1991.45.1.47

Li M, Yoo CG, Pu Y, Ragauskas AJ (2018) 31P NMR chemical shifts of solvents and products impurities in biomass pretreatments. ACS Sustain Chem Eng 6(1):1265–1270. https://doi.org/10.1021/acssuschemeng.7b03602

Malutan T, Nicu R, Popa VI (2008) Contribution to the study of hydroxymetylation reaction of alkali lignin. BioResources 3(1):13–20. https://doi.org/10.15376/biores.3.1.13-20

Marton J, Marton T, Falkehag SI, Adler E (1966) Alkali-Catalyzed Reactions of Formaldehyde with Lignins. In: Marton J (ed) Lignin Structure and Reactions. American Chemical Society, Washington

Meng X, Crestini C, Bem H, Hao N, Pu Y, Ragauskas AJ, Argyropoulos DS (2019) Determination of hydroxyl groups in biorefinery resources via quantitative 31P NMR spectroscopy. Nat Protoc 14(9):2627–2647. https://doi.org/10.1038/s41596-019-0191-1

Mishra PK, Ekielski A (2019) The self-assembly of lignin and its application in nanoparticle synthesis: a short review. Nanomaterials 9:243–258. https://doi.org/10.3390/nano9020243

Muller PC, Glasser WG (1984) Engineering plastics from lignin VIII phenolic resin prepolymer synthesis and analysis. J Adhes 17(2):157–173. https://doi.org/10.1080/00218468408079672

Nicolau VV, Estenoz DA, Meira GR (2013) Hydroxy-methylation of phenol revisited: a readjusted mathematical model. Ind Eng Chem Res 52:18140–18152. https://doi.org/10.1021/ie401231w

Olivares M et al (1988) Kraft lignin utilization in adhesives. Wood Sci Technol 22(2):157–165. https://doi.org/10.1007/BF00355851

Paananen H, Pakkanen TT (2020) Kraft lignin reaction with paraformaldehyde. Holzforschung 74(7):663–672. https://doi.org/10.1515/hf-2019-0147

Paananen H, Alvila L, Pakkanen TT (2021) Hydroxy-methylation of softwood kraft lignin and phenol with paraformaldehyde. Sustain Chem Pharm 20:100376–100383. https://doi.org/10.1016/j.scp.2021.100376

Peng W, Riedl B, Barry AO (1993) Study on the kinetics of lignin methylolation. J Appl Polym Sci 48(10):1757–1763. https://doi.org/10.1002/app.1993.070481009.Rivlin

Peng W, Barry AO, Riedl B (1992) Characterization of methylolated lignin by H-Nmr and 13C-Nmr. Nmr J Wood Chem Technol 12(3):299–312. https://doi.org/10.1080/02773819208545236

Rivlin M, Eliav U, Navon G (2015) NMR studies of the equilibria and reaction rates in aqueous solutions of formaldehyde. J Phys Chem B 119(12):4479–4487. https://doi.org/10.1021/jp513020y

Ruwoldt J, Tanase-opedal M, Syverud K (2022) Ultraviolet spectrophotometry of lignin revisited: exploring solvents with low harmfulness, lignin purity, hansen solubility parameter, and determination of phenolic hydroxyl groups. ACS Omega 7(50):46371–46383. https://doi.org/10.1021/acsomega.2c04982

Sette M, Wechselberger R, Crestini C (2011) Elucidation of lignin structure by quantitative 2D NMR. Chem Eur J 17(34):9529–9535. https://doi.org/10.1002/chem.201003045

Taverna ME et al (2015) Mechanical evaluation of laminates based on phenolic resins using lignins as partial substitutes for phenol. BioResources 10(4):8325–8338

Taverna ME et al (2017) Effect of kraft lignin from hardwood on viscoelastic, thermal, mechanical and aging performance of high pressure laminates. Waste Biomass Valoriz 10(3):585–597. https://doi.org/10.1007/s12649-017-0088-6

Taverna ME, Felissia F, Area MC, Estenoz DA, Nicolau VV (2019) Hydroxy-methylation of technical lignins from South American sources with potential use in phenolic resins. J Appl Polym Sci 136(26):47712–47724. https://doi.org/10.1002/app.47712

Vallejos ME, Kruyeniski J, Area MC (2017) Second-generation bioethanol from industrial wood waste of South American species. Biofuel Research Journal 15:654–667. https://doi.org/10.18331/BRJ2017.4.3.4

Vázquez G et al (1997) Effect of chemical modification of lignin on the gluebond performance of lignin-phenolic resins. Bioresour Technol 60(3):191–198. https://doi.org/10.1016/S0960-8524(97)00030-8

Vázquez G et al (1999) Acetosolv pine lignin as copolymer in resins for manufacture of exterior grade plywoods. Bioresour Technol 70(2):209–214. https://doi.org/10.1016/S0960-8524(99)00020-6

Wells T, Kosa M, Ragauskas AJ (2013) Polymerization of Kraft lignin via ultrasonication for high-molecular- weight applications. Ultrason Sonochem 20(6):1463–1469. https://doi.org/10.1016/j.ultsonch.2013.05.001

Yang S, Zhang Y, Yuan TQ, Sun RC (2015) Lignin-phenol-formaldehyde resin adhesives prepared with biorefinery technical lignins. J Appl Polym Sci 132(36):42493–42501. https://doi.org/10.1002/app.42493

Zhao LW, Griggs BF, Chen CL, Gratzl JS, Hse CY (1994) Utilization of softwood kraft lignin as adhesive for the manufacture of reconstituted wood. J Wood Chem Technol 14(1):127–145. https://doi.org/10.1080/02773819408003090

Authors and Affiliations

Micaela B. Peralta[1,2] · Nicolò Pajer[3,4] · Claudia Crestini[3,4] · Verónica V. Nicolau[1,2]

✉ Claudia Crestini
claudia.crestini@unive.it

✉ Verónica V. Nicolau
vnicolau@facultad.sanfrancisco.utn.edu.ar

[1] GPol, Departamento de Ingeniería Química, Facultad Regional San Francisco, Universidad Tecnológica Nacional, Av. de la Universidad 501, San Francisco, Córdoba, Argentina

[2] Consejo Nacional de Investigaciones Científicas y Técnicas (CONICET), Godoy Cruz 2290, CABA Buenos Aires, Argentina

[3] Department of Molecular Sciences and Nanosystems, Ca' Foscari University of Venice, Via Torino 155, 30172 Venice-Mestre, Italy

[4] Center for Colloid and Surface Science, Via Della Lastruccia 3, 50019 Sesto Fiorentino (Florence), Italy